

# Light Response of Poly(ethylene 2,6-naphthalate) to Neutrons

Brennan Hackett<sup>a,b,\*</sup>, Richard deBoer<sup>c</sup>, Yuri Efremenko<sup>a,b</sup>, Michael Febbraro<sup>b</sup>, Jason Nattress<sup>b</sup>, Dan Bardayan<sup>c</sup>, Chevelle Boomershine<sup>c</sup>, Kristyn Brandenburg<sup>d</sup>, Stefania Dede<sup>c,e</sup>, Joseph Derkin<sup>d</sup>, Ruoyu Fang<sup>c</sup>, Adam Fritsch<sup>d,f</sup>, August Gula<sup>c</sup>, Gyürky György<sup>g</sup>, Gula Hamad<sup>d</sup>, Yenuel Jones-Alberty<sup>d</sup>, Beka Kelmar<sup>c</sup>, Khachatur Manukyan<sup>c</sup>, Miriam Matney<sup>c</sup>, John McDonaugh<sup>c</sup>, Shane Moylan<sup>c</sup>, Patrick O'Malley<sup>c</sup>, Shahina Shahina<sup>c</sup>, Nisha Singh<sup>d</sup>

<sup>a</sup>*Department of Physics and Astronomy, University of Tennessee, Knoxville Tennessee, USA*

<sup>b</sup>*Oak Ridge National Laboratory, Oak Ridge, TN, USA*

<sup>c</sup>*Department of Physics and the Joint Institute for Nuclear Astrophysics, Notre Dame, Indiana 46556, USA*

<sup>d</sup>*Edwards Accelerator Laboratory, Department of Physics and Astronomy, Ohio University, Athens, Ohio 45701, USA*

<sup>e</sup>*Cyclotron Institute, Texas A&M University, College Station, Texas, United States, 77843*

<sup>f</sup>*Department of Physics, Gonzaga University, Spokane, Washington 99258, USA*

<sup>g</sup>*Institute of Nuclear Research (ATOMKI), Hungarian Academy of Sciences, Debrecen, Hungary*

---

## Abstract

There is increasing necessity for low background active materials as ton-scale, rare-event and cryogenic detectors are developed. Poly(ethylene-2,6-naphthalate) (PEN) has been considered for these applications because of its robust structural characteristics, and its scintillation light in the blue wavelength region. Radioluminescent properties of PEN have been measured to aid in the evaluation of this material. In this article we present a measurement of PEN's quenching factor using three different neutron sources; neutrons emitted from spontaneous fission in  $^{252}\text{Cf}$ , neutrons generated from a DD generator, and neutrons emitted from the  $^{13}\text{C}(\alpha,n)^{16}\text{O}$  and the  $^7\text{Li}(p,n)^7\text{Be}$  nuclear reactions. The fission source used time-of-flight to determine the neutron energy, and the neutron energy from the nuclear reactions was defined using thin targets and reaction kinematics. The Birk's factor and scintillation efficiency were found to be  $kB = 0.12 \pm 0.01 \text{ mm MeV}^{-1}$  and  $S = 1.31 \pm 0.09 \text{ MeV}_{ee} \text{ MeV}^{-1}$  from a simultaneous analysis of the data obtained from the three different sources. With these parameters, it is possible to evaluate PEN as a viable material for large-scale, low background physics experiments.

**Keywords:** poly(ethylene 2,6-naphthalate), PEN, Birk's factor

---



---

\*Corresponding author

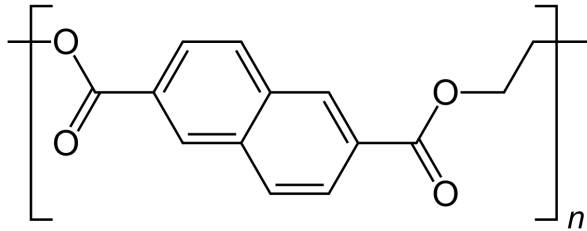


Figure 1: Skeleton structure of the repeating unit for the polymer PEN.

## 1. Introduction

The next generation of rare-event physics experiments continue to pursue quasi-background free environments in ton-scale detectors [1, 2, 3]. This is being achieved through improvements in spatial and temporal background rejection, particle identification capabilities, higher active veto system efficiency, and developments in ultra-low background materials.

Poly(ethylene 2,6-naphthalate) (PEN), is of interest as a low background, active material in rare-event and multi-ton liquid argon experiments [3, 4]. PEN is an aromatic polyester (Fig. 1) that exhibits excellent mechanical strength, chemical resistance, scintillates and wavelength shifts VUV light. PEN is a unique polymer in that it scintillates inherently, with its primary scintillation light in the blue region ( $\sim 400$  nm), therefore, unlike traditional plastic scintillators, no additional fluors are required [4].

For active veto applications in low background experiments, it is important to fully understand PEN's ability to veto radioactive decays, which may occur inside or on the surface of a PEN component (e.g. products of radon decays). This can be understood through Monte Carlo simulations of the radioactive decays and the light propagating in the active veto system, allowing for the full characterization of the active veto system performance. The light response for PEN has been measured for alpha particles [5], but never for neutron interactions. Quenching in scintillators is defined by considering the light produced by a nuclear recoil,  $L(E)_{nr}$  as a fraction of the light produced by an electronic recoil of equivalent energy,  $L(E)_{er}$ :

$$QF(E) = \frac{L(E)_{nr}}{L(E)_{er}}. \quad (1)$$

There are many models to describe how the light is quenched as a function of energy in a scintillator [6]. This paper will focus on the use of Birk's law:

$$\frac{dL}{dr} = S \frac{\frac{dE}{dr}}{1 + kB \frac{dE}{dr}}. \quad (2)$$

Birk's law describes how the light per unit length,  $\frac{dL}{dr}$ , is quenched as a function of stopping power,  $\frac{dE}{dr}$ . The scintillation efficiency  $S$ , and the Birk's constant,  $kB$ , describes the shape of the light response curve, and to what degree it is non-linear as a function of energy deposition by the neutron.

To determine the quenching factors and determine the Birk's parameters, it is necessary to determine which measured events are from neutrons scattering and generating a nuclear recoils, and which are from  $\gamma$ -ray interactions with electrons. One tool used for this is pulse shape discrimination (PSD) as it allows the distinction between particles with different charge/mass ratios, such as electron and proton recoils. Fig. 2 defines the pulse shape discrimination parameter as the fraction of the integral of the light pulse tail compared to the integral of the whole light pulse from the detector. This is the result of the population of different singlet and triplet excited states by electron and nuclear recoils. Examples of average light pulses at a light yield of 0.6 MeV electron equivalent, or MeVee, are shown for PEN in Fig. 2.

This paper is organized as follows; Section 2 provides details about the PEN scintillation detector used for this measurement; followed by Section 3 which describes the experimental preparation and procedure for the neutron measurements. It also includes a description of the calibration method for the measurements, this is followed by a brief description of the error analysis method in Section 4. Finally, Section 5 presents the findings for the quenching

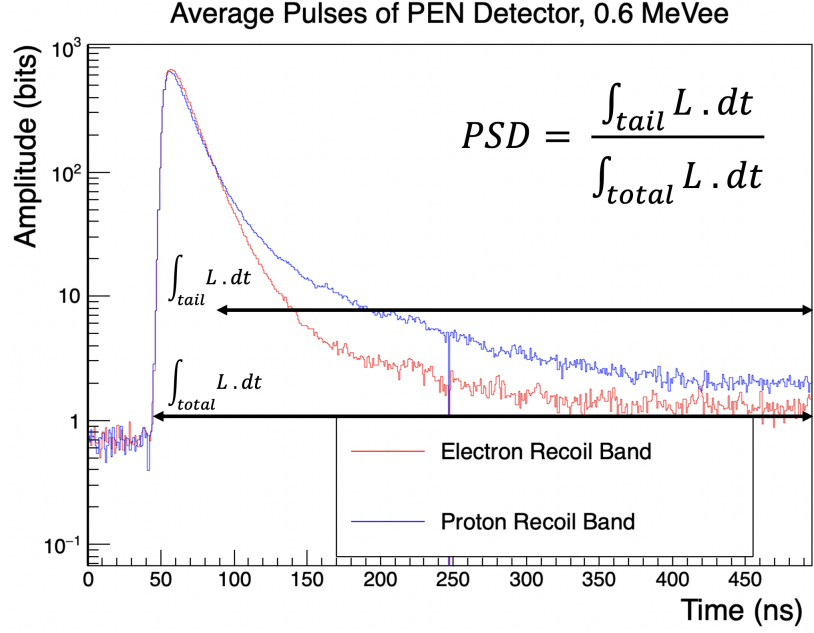


Figure 2: Average pulses in PEN for electron and proton recoils for 100 pulses. Pulse energies are approximately 0.6 MeVee.

factor and Birk's constant for PEN and summarizes the results of this study.

## 2. PEN scintillation detector

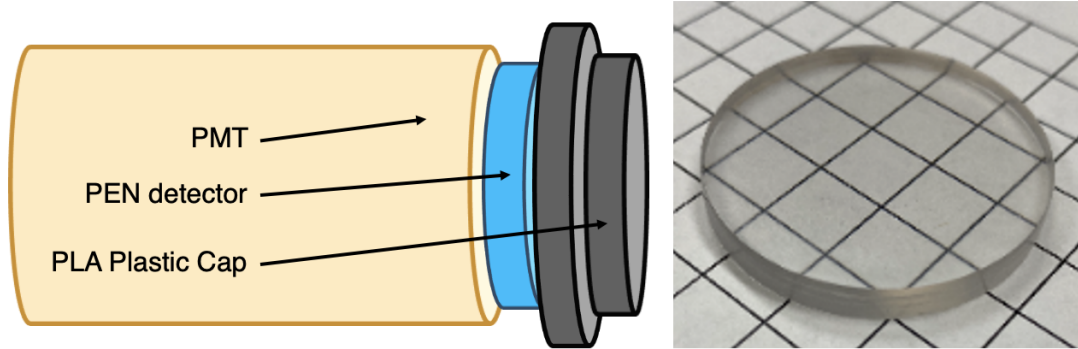


Figure 3: The PEN component used for these luminescent measurements has a radius of 5.08 cm and a thickness of 0.5 cm.

PEN is a semi-crystalline aromatic polymer which co-exists in both the crystalline and amorphous phases [4]. The PEN component used for this measurement is an amorphous

sample produced by an injection molding process described in Ref. [4]. The commercially available PEN used to produce this component was supplied by Teonex, TN-8065S. The PEN component is 5.08 cm in diameter and 0.5 cm thick (Fig. 3). The detector consisted of three main components; a 3D printed cap to hold the PEN component and optically seal the detector, the PEN component itself, and a photomultiplier tube (PMT). For the measurement conducted using nuclear reaction neutrons, a Hamamatsu R6233 2" PMT was used. This tube is a hybrid design with box-and-grid technology to maximize light collection, and linear focused technology to improve pulse linearity [7]. For the measurement conducted using spontaneous fission neutrons, a Hamamatsu R7224 2" PMT was used. This tube has a linear focused design, with a smaller transient time spread and larger gain, resulting in a lower light threshold and improved time resolution, and therefore energy resolution. The same detector used for the fission chamber measurement was used in the DD generator measurement. Both detectors were lined with Teflon which serves as the optical reflector, and the component was optically coupled to the face of the PMT using Saint Gobain optical coupling compound, BC-630.

### 3. Experimental Method

The experimental method was as follows;  $L(E)_{er}$  was calibrated for each detector with gamma-ray sources. Next, the energy of the neutrons are determined using reaction kinematics or time-of-flight. Finally, the quenching factor is determined by measuring the light produced for a proton recoil of a given neutron energy,  $L(E)_{pr}$ .

#### 3.1. Detector Calibration

Gamma-ray radiation sources were used to calibrate the PEN scintillation detector in each measurement. The gamma-ray energies from these sources have an energy range  $0.356 \leq E_\gamma \leq 1.332$  MeV. The gamma-ray source response in the PEN scintillation detector was

simulated in Geant4, and the energy deposited by recoiling electrons in the PEN component was recorded. The experimental resolution of the calibration source data was recreated in the simulation data (Fig. 5) using Gaussian smearing with the resolution (Eq. 3), and the inverse error function (Eq. 4):

$$FWHM = E * \sqrt{\alpha^2 + \frac{\beta^2}{E}} \quad (3)$$

$$E' = (E + erf^{-1}(r) * \sqrt{2 \left( \frac{FWHM}{2.35} \right)^2}) * C. \quad (4)$$

To determine the optimal  $\alpha$  and  $\beta$  parameters, first a Gaussian function is fit to the Compton edge in the data.

$$f(x) = k * \exp^{-\frac{1}{2} \left( \frac{x-\mu}{\sigma} \right)^2} \quad (5)$$

The initial values for  $\mu$  and  $\sigma$  were estimated in the Gaussian function (Eq. 5) and then fit to the simulation. The simulation is multiplied by a scaling factor,  $C$ , to reproduce the simulation on the same scale as the data, which is in arbitrary units. An iterative method was applied to find optimal parameters for  $\alpha$ ,  $\beta$ , and  $C$ . A minimum  $\chi^2$  is found between the fit function and smeared simulated deposited energy spectrum, and used to quantify the quality of the fit.

Figure 4 shows an example of a best fit for a  $^{137}\text{Cs}$  source in comparison with the data. The simulation was smeared with the following values;  $\alpha = 0.053$ ,  $\beta = 0.12$  and  $C = 8020$ . The same  $\alpha$  and  $\beta$  parameters were then used to Gaussian smear the neutron simulations to determine the neutron edge.

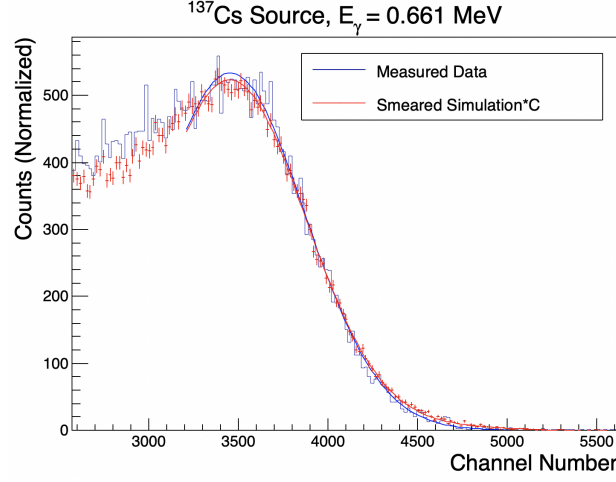


Figure 4: The measured data of a  $^{137}\text{Cs}$  source with  $E_\gamma = 0.662$  MeV, impinging on a PEN scintillation detector is shown in blue, and fit with a Gaussian (Eq. 5). The simulation is shown in red, also fit with a Gaussian, and the statistics are normalized to the data. The Gaussian smearing (Eq. 3 and Eq. 4) is applied with the following values;  $\alpha = 0.053$ ,  $\beta = 0.12$  and  $C = 8020$ .

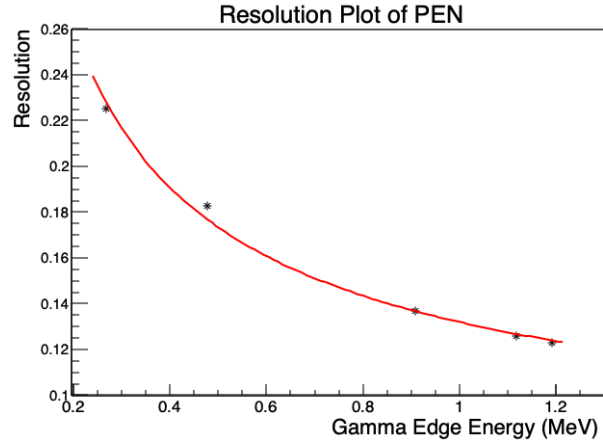


Figure 5: The detector energy resolution was measured using various gamma-ray sources. This plot shows the detector resolution defined as  $\frac{FWHM}{L}$ , for the detector used at the University of Notre Dame for the nuclear reaction neutron sources.

### 3.2. Calibration of Neutron Sources and Experimental Setup

Any single neutron source measurement could result in systematic errors in the measured light response, and would be limited in its energy range. However, by measuring the luminescent response of PEN using multiple neutron sources, as well as using different light collection systems and data acquisition systems, agreement between measurements will reduce the likelihood of global systematic errors. Therefore three different types of neutron sources were used; a white  $^{252}\text{Cf}$  neutron source with time-of-flight, monoenergetic neutrons from a DD generator, and monoenergetic neutrons produced from the  $^{13}\text{C}(\alpha, n)^{16}\text{O}$  and  $^7\text{Li}(p, n)^7\text{Be}$  reactions using monoenergetic particle beams, made incident on thin targets where the beam experienced very small energy losses. There are different methods used to determine the neutron energies between these three measurements. The first is time of flight, where the flight time,  $T$  of a neutron can be used to determine its kinetic energy,  $E_n$  from a white neutron source, by knowing the distance it travels,  $D$ , and the mass of the neutron,  $m_n$ . The neutron's energy and its uncertainty can be found using the following equations:

$$E_n = \frac{1}{2}m_n \left(\frac{D}{T}\right)^2 \quad (6)$$

$$\frac{\Delta E_n}{E_n} = 2\sqrt{\left(\frac{\Delta D}{D}\right)^2 + \left(\frac{\Delta T}{T}\right)^2}. \quad (7)$$

The energy resolution of this measurement is defined by the uncertainty in the time and distance. It is possible to increase the flight path to improve the energy resolution, but this comes at the cost of statistics. Additionally, as the neutron energy increases, its time-of-flight decreases, therefore resulting in a decrease in energy resolution. This places an upper limit on the energies that can be reasonably measured using time-of-flight.

The second method used to determine the neutron's energy is to use reaction kinematics. Neutrons produced in two-body nuclear reactions will have a well defined energy depending



on the beam bombarding energy and the angle of emission, with an energy uncertainty determined by the solid angle acceptance, energy loss through the target and fluctuation in the beam energy. Both the beam energy fluctuations and the energy loss through the target were determined to be negligible. There are potentially other open reaction channels that produce large numbers of background events. PSD can be used to remove background events by distinguishing between proton and electron recoils, but the separation becomes worse at lower energies. Using this method, there is a limited ability to measure neutrons at energies less than  $\approx 0.7$  MeV.

### *3.2.1. $^{252}\text{Cf}$ Spontaneous Fission Source*

For this measurement,  $^{252}\text{Cf}$  was used as a white neutron source. The non-relativistic kinetic energy of the neutrons was determined using time-of-flight from the source to the detector. Neutrons are produced by spontaneous fission in  $^{252}\text{Cf}$ . When a fission spontaneously occurs, both neutrons and photons are released. The  $^{252}\text{Cf}$  source is within a small fission chamber, which will trigger on fissile material being released, and therefore will set a start time for the event [8]. The  $^{252}\text{Cf}$  source is plated on a platinum disk and is set parallel to the signal collector. The  $^{252}\text{Cf}$  source and signal collector are set in a hemispherical ionization chamber filled with a mixture of 97% Ar and 3%  $\text{CO}_2$  gas.

The trigger from the ionization chamber is fed into a CAEN desktop digitizer model 5730, and coincidence is required between the fission chamber and PEN scintillation detector to record the event. The time of the trigger was defined by using the CAEN onboard Leading Edge Discriminator, or LED [9]. Though using an LED may result in edge walking for varying pulse amplitudes, this was not a concern for the fission chamber pulses, as the rise time was faster than the digitizer sampling speed. The PEN scintillation detector had pulses with significantly slower rise times, therefore on board CFD (constant fraction discriminator), triggering at 50% amplitude, was used to determine the start time of the pulse. The distance between the fission chamber and the PEN scintillation detector was

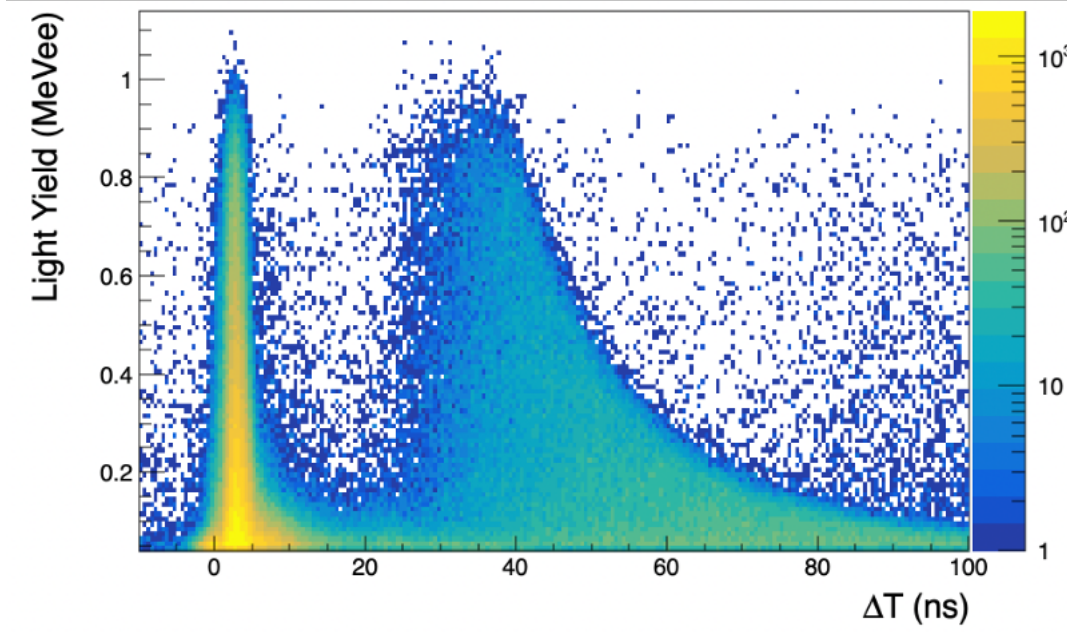


Figure 6: The time of flight was used to determine the energy of neutrons from the  $^{252}\text{Cf}$  source. This plot shows the time of flight or  $\delta T$  for events from the fission chamber to the PEN scintillation detector versus the light yield for that event. The gamma flash can be seen focused around  $\sim 3$  ns.

measured to be  $D = 0.890 \pm 0.005$  m. The gamma flash time of flight in PEN was centered at  $\delta T = 2.8$  ns, with a resolution of  $FWHM = 2.3$  ns. This resolution was used to determine the neutron energy resolution, as shown in Eq. 7. This is very close to the resolution of channel-to-channel timing using the onboard CAEN DPP-PSD firmware ( $\sim 2.2$  ns) [9]. The total pulse was integrated over 430 ns, with the short integral starting at an offset of 70 ns from the peak amplitude of the pulse. The pulse shape discrimination parameter, described in Fig. 2, was defined by using the ratio of the total pulse and the short integral (Fig. 7). Averages of PEN scintillation pulses for the electronic and nuclear recoils are also shown in Fig. 2.

Using a similar technique that was used for the gamma calibration of the PEN scintillation detectors, the energy deposited by recoiling protons in a PEN component was simulated using Geant4. The simulation is smeared using the same smearing function as shown in Eq. 4, with the resolution (FWHM) being defined by Eq. 3.

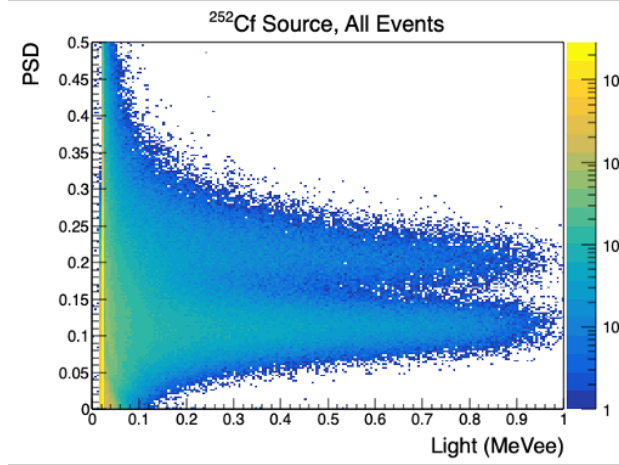


Figure 7: This plot shows the PSD for the PEN scintillation detector used in the fission chamber measurements. The neutron events and therefore proton recoils can be seen in the top band and the gamma events and therefore electronic recoils can be seen in the bottom band.

Energy deposited by neutrons in hydrogen-based scintillators has a step shape, that can be fit with a sigmoid function:

$$f(x) = \frac{p_0}{1 + e^{-p_1(x-p_2)} + x * p_3}. \quad (8)$$

This sigmoid function was fit to the data, to determine the parameters  $p_1$  and  $p_2$ . With these parameters fixed, and  $p_0$  and  $p_3$  allowed to float, the sigmoid function was again fit but this time to the simulation. The simulation was scaled by a “quenching factor” or QF. The  $\chi^2$  for this fit was minimized by varying the QF. The accuracy of the quenching factor was defined by the variation of the QF as the  $\chi^2$  per degrees of freedom, or  $\Delta \frac{\chi^2}{DOF} = 2$ .

The width of the energy step for the fission chamber measurements was determined by the timing resolution of the experiment, or the FWHM of the gamma pulse. This is equivalent to a FWHM resolution of 36 keV for a 1 MeV neutron. The energy steps for neutrons had a range that was larger or equivalent to the energy resolution from the timing. The range of neutron energies measured from the  $^{252}\text{Cf}$  source was  $0.5 \leq E_n \leq 2.0$  MeV.

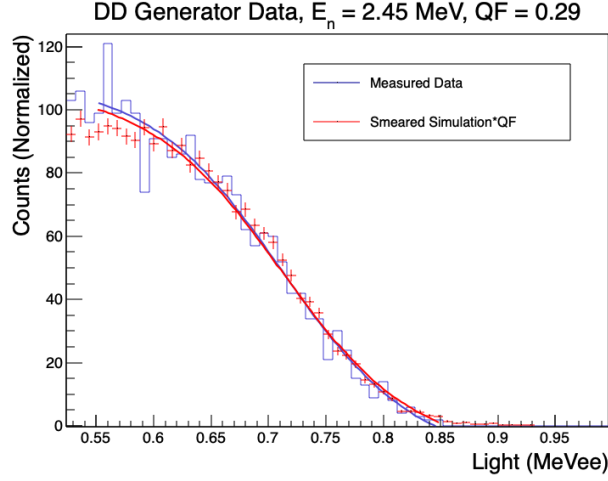


Figure 8: The measurement of neutrons from a DD generator is shown in blue, and fit with a sigmoid function, also in blue (Eq. 8). The smeared simulation for neutrons of  $E_n = 2.45$  MeV is plotted in red, and scaled to the statistics of the data. The red line shows the simulation fit to the same sigmoid function as the data.

### 3.2.2. DD Generator

A DD generator uses the fusion of deuterium to produce neutrons, as described in Eq. 9:



This reaction releases monoenergetic neutrons at  $E_n = 2.45$  MeV [10]. Because this source is monoenergetic, time-of-flight was not needed to determine the energy of the neutrons. The data was collected on the same CAEN 5730 desktop digitizer used in the  ${}^{252}\text{Cf}$  fission source measurements. The total pulse was integrated over 430 ns, with the short integral starting at an offset of 70 ns from the peak amplitude of the pulse.

The data for the DD measurement was also fit with the sigmoid function (Eq. 8). These simulations were generated in Geant4, and the energy deposited on protons from 2.45 MeV neutrons was recorded. The simulation was then smeared as described in Eq. 4. The data and smeared simulation are shown in Fig. 8.

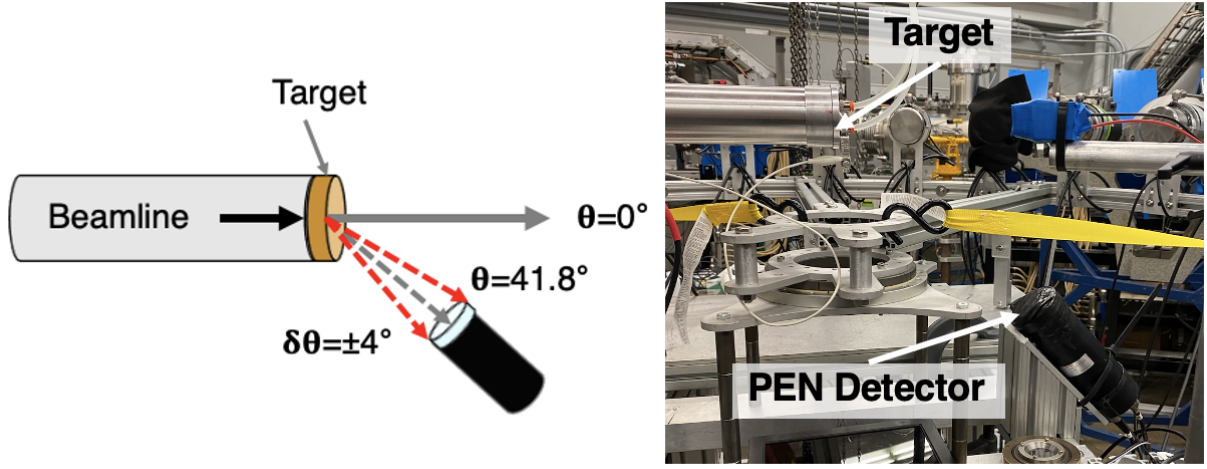


Figure 9: Experimental setup at University of Notre Dame Nuclear Science Laboratory with a diagram (left) and image (right). Detector was placed 30 cm from the target, at an angle of  $41.8^\circ$  from the beamline.

### 3.2.3. Nuclear Reaction Neutrons

The nuclear reactions used in these measurements were  ${}^7\text{Li}(p,n){}^7\text{Be}$  and  ${}^{13}\text{C}(\alpha,n){}^{16}\text{O}$ , and were conducted at the University of Notre Dame Nuclear Science Laboratory. The Sta. ANA 5 MV accelerator was used to produce a beam of  ${}^1\text{H}^+$ ,  ${}^4\text{He}^+$  or  ${}^4\text{He}^{++}$ , which was impinged onto a water-cooled target. For the  ${}^7\text{Li}(p,n){}^7\text{Be}$  measurement, a beam of  ${}^1\text{H}^+$  was impinged on a thin LiF foil (natural abundance) mounted onto a thick tantalum backing. For the  ${}^{13}\text{C}(\alpha,n){}^{16}\text{O}$  reaction, a beam of either  ${}^4\text{He}^+$  or  ${}^4\text{He}^{++}$  was impinged on a 99% isotopically enriched  ${}^{13}\text{C}$  layer evaporated on a thick tantalum backing. The outgoing neutrons for both reactions were measured at angles  $\theta = 41.8^\circ$  or  $127.5^\circ$  in the laboratory frame. The experimental set up at  $\theta = 41.8^\circ$  is shown in Fig. 9.

Waveforms taken from the PEN scintillation detector were recorded using a CAEN V1725 250 MS/s, 14-bit waveform digitizer. The total pulse was integrated over 440 ns, with the short integral being 340 ns long and starting at an offset of 80 ns from the peak amplitude of the pulse.

The  ${}^7\text{Li}(p,n){}^7\text{Be}$  reaction was used to measure neutrons in the range of  $0.8 \leq E_n \leq$

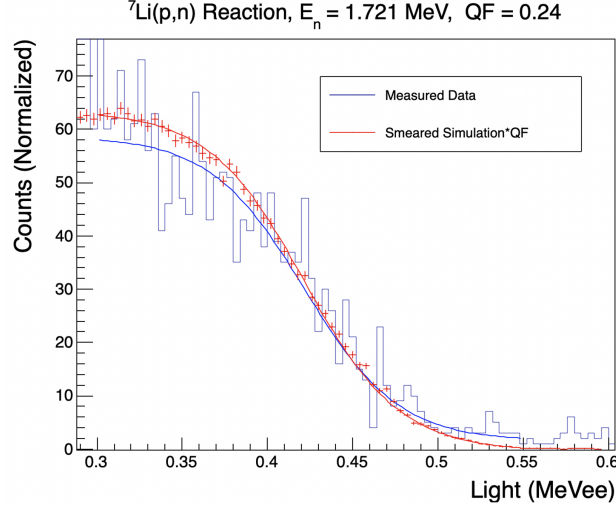


Figure 10: The data from  $E_n = 1.724$  MeV is plotted in blue with a sigmoid function (Eq. 8). The simulation is plotted in red, fit with a sigmoid function and normalized to the statistics of the data. The data has excellent agreement with the simulation over the range where the sigmoid function is fit.

1.9 MeV and the  $^{13}\text{C}(\alpha, n)^{16}\text{O}$  reaction was used to measure neutrons in the range of  $2.5 \leq E_n \leq 7.1$  MeV. The energy deposited by an equivalent energy neutron was simulated using Geant4 for each measurement. As described in Section 3.2.1, the data was fit with a sigmoid function, the terms  $p_1$  and  $p_2$  were fixed, and the sigmoid function was fit to the smeared neutron simulation. In Fig. 10, the data from  $E_n = 1.724$  MeV is plotted with the corresponding simulation. The PSD gates were determined by projecting a light bin onto the PSD axis and fitting a double Gaussian for each the proton and electron recoil band (Fig. 11). The PSD gates were then defined to be  $2\sigma$  from the mean of the Gaussian for each recoil band. The use of the PSD gates were vital in minimizing background events in the nuclear reaction measurements as the gamma-ray background was often significant. An example is in the  $^{13}\text{C}(\alpha, n)^{16}\text{O}$  reaction, if the beam energy is  $E > 3.9$  MeV, then the second excited state of  $^{16}\text{O}$  is populated, and will result in the emission of a  $\sim 6$  MeV gamma-ray. This high-energy gamma-ray is one example of potential backgrounds that could effect the measurements.

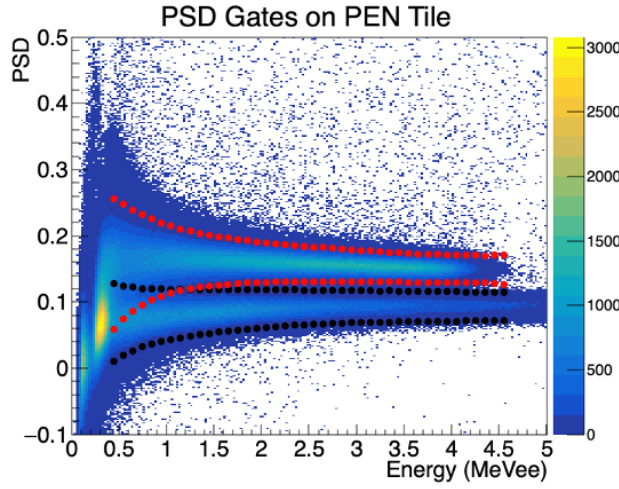


Figure 11: This plot shows the PSD gates for the PEN scintillation detector. Gates were used to distinguish neutron and gamma-ray events with an estimated probability of  $2\sigma$ .

#### 4. Error Analysis

The accuracy of the neutron energy determination for the fission chamber measurements was determined by measuring the spread of energies for a given energy slice. This was done by calculating the root mean squared of all the neutron energies of a certain slice:

$$RMS = \sqrt{\frac{\sum_{i=1}^n (E_i - E_{Avg})^2}{n}}. \quad (10)$$

The accuracy in the energy for the nuclear reaction measurements was partially determined by the kinematic acceptance of the detector geometry. It was also impacted by variations in the beamline energy impinging on the target, which was less than 40 keV between runs.

The error in the quenching factor values has been determined by variation seen in  $\Delta_{\frac{\chi^2}{DOF}} = 2$ , where  $\chi^2$  is found by fitting the sigmoid function to the neutron edge.

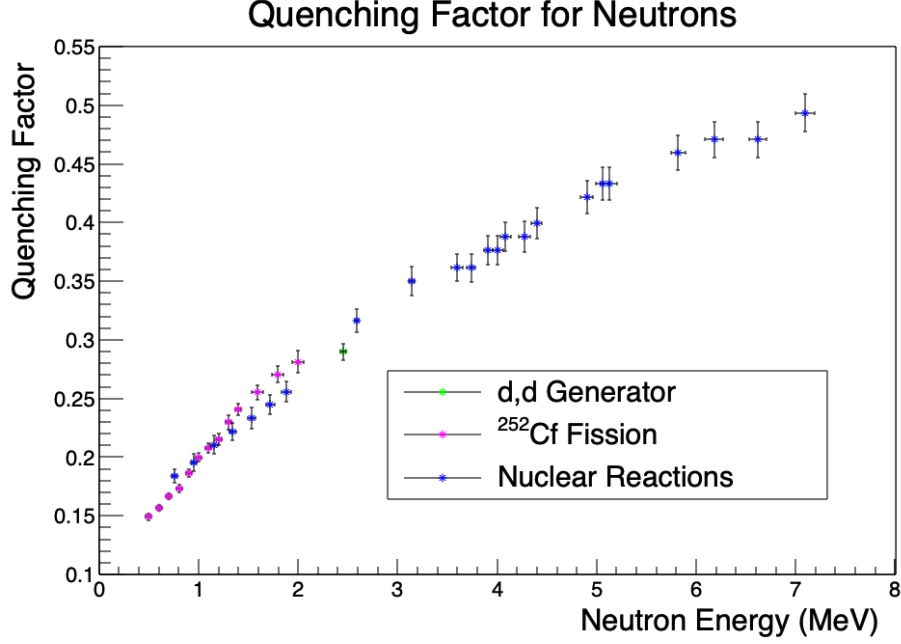


Figure 12: This plot shows the quenching factor of PEN as a function of energy. Quenching factors of all data show good agreement with each other.

## 5. Results

The quenching factors are plotted for the three measurement methods in Fig. 12. It is seen that all three measurements have a good agreement with each other and follow a similar trend. At  $E_n = 1.0$  MeV, PEN has a quenching factor  $QF = 0.199 \pm 0.005$ . Comparing to the commercial scintillator EJ-200, at  $E_n = 1.0$  MeV, its quenching factor is  $QF = 0.156 \pm 0.003$  [11]. The reason for the reduced light quenching in PEN is unclear, but it does lend itself as a promising property for PEN as a self-vetoing material. It suggests that for nuclear recoils, the percentage of light quenched in PEN will be less than it is in the commercial scintillator EJ-200.

By using numerical integration, it is possible to analytically fit the Birk's law to quenching factor data using Eq. 2. A best fit for the PEN light response was found and values for the scintillation efficiency,  $S$  and the Birk's factor,  $k_B$  were derived. The ROOT Minuit fitting function determined the parameters which provided a minimum  $\chi^2$  and their respective



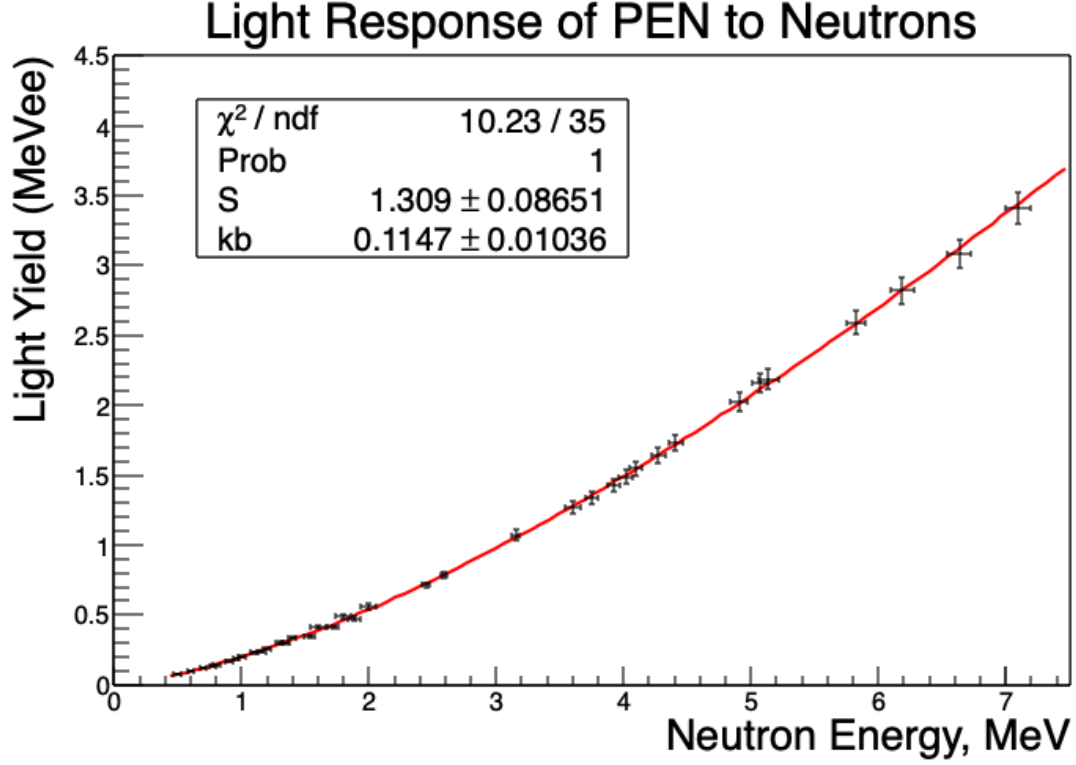


Figure 13: The light response of PEN, globally fit with Birk's function, as described in Eq. 2. The parameters were found to be  $kB = 0.12 \pm 0.01 \text{ mm MeV}^{-1}$  and  $S = 1.31 \pm 0.09 \text{ MeV}_{ee} \text{ MeV}^{-1}$ .

error, for a global fit.

As shown in Fig. 13, the light response of PEN was fit with Birk's equation with a final fit of  $kB = 0.12 \pm 0.01 \text{ mm MeV}^{-1}$  and  $S = 1.31 \pm 0.09 \text{ MeV}_{ee} \text{ MeV}^{-1}$ . These parameters describe the shape of the quenching factor and its value for a given energy. The larger the  $kB$ , the more the light response becomes non-linear.

Using this measured neutron response of PEN, the shape of neutrons from the  $^{13}\text{C}(\alpha, n)^{16}\text{O}$  reaction where  $E_n = 4.91 \text{ MeV}$ , was recreated using Geant4. By defining the Birk's factor and scintillation efficiency, it is possible to define quenching factors for PEN at all energies. In Fig. 14, the simulated energy deposited by the neutrons are smeared and scaled given the light response of PEN. It is clear that over the whole spectrum, there is strong agreement and the method used in this analysis does well to recreate the measured data.

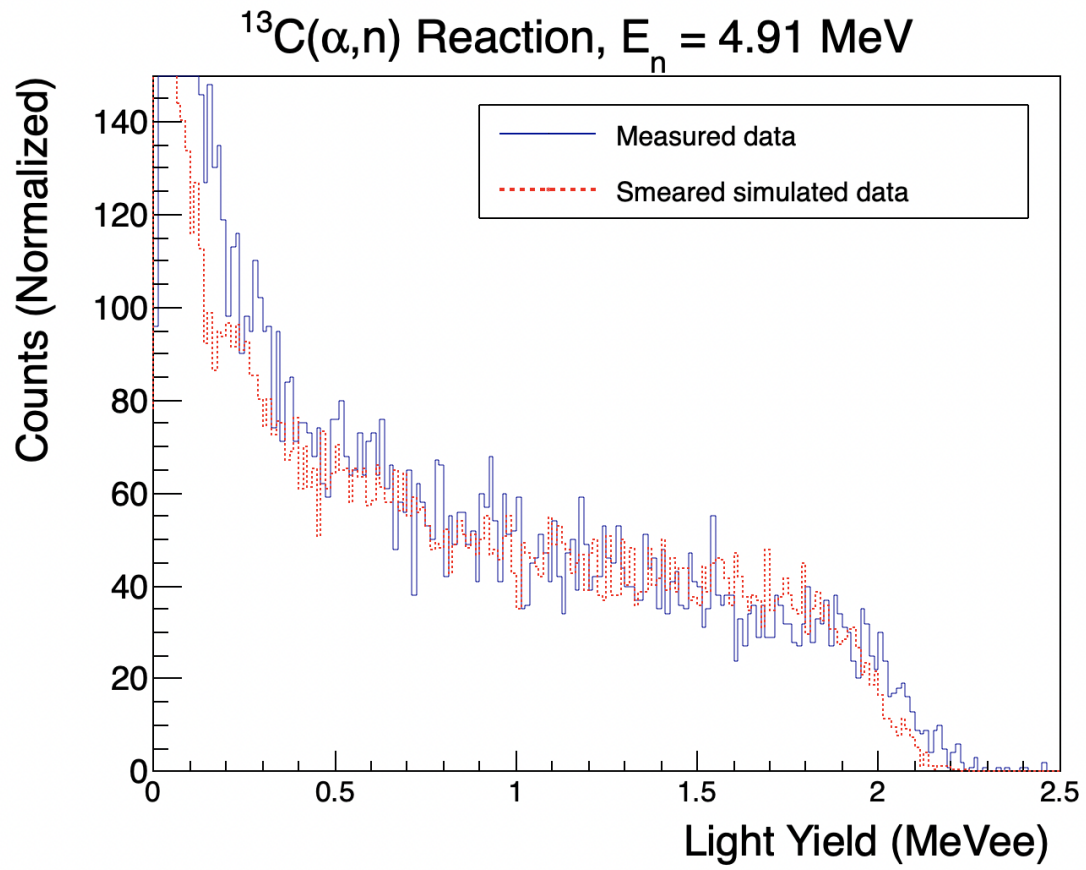


Figure 14: This figure shows data taken from neutrons generated in nuclear reactions,  $E_n = 4.91 \text{ MeV}$ . The simulated energy deposited by neutrons at 4.906 MeV are smeared and scaled given the light response of PEN, recreating the measured data.

## 6. Conclusion

PEN has been identified as a material of interest for ton-scale physics experiments, for its inherent scintillation at  $\lambda \approx 450$  nm and its wavelength shifting capabilities for VUV light. For applications in quasi background-free environments, PEN must act as a self-vetoing material and the light response of PEN is necessary information to understand a PEN component's veto efficiency and therefore its effectiveness. The use of multiple neutron sources allows for the measurement of the light response of PEN over a large neutron energy range, with each measurement method having its own benefits. Pulse shape discrimination was used to separate gamma and neutron events occurring in the detector. This was particularly of use when using nuclear reactions at an accelerator as a source of neutrons, due to large backgrounds related to the reaction. The Birk's law was fit to the light response of PEN and the Birk's factor was determined to be  $kB = 0.12 \pm 0.01$  mm MeV<sup>-1</sup> and the scintillation efficiency is  $S = 1.31 \pm 0.09$  MeV<sub>ee</sub> MeV<sup>-1</sup>. With these parameters determined, it is now possible to evaluate PEN for low-background and ton-sale applications and to determine its viability in vetoing background events.

## Acknowledgements

his research was partially supported by the National Science Foundation through Grant No. PHY-1713857 and PHY-2011890, and the Joint Institute for Nuclear Astrophysics through Grant No. PHY-1430152 (JINA Center for the Evolution of the Elements). It was partially supported by NKFIH grant No. K134197 and provided by the U.S. Department of Energy, Office of Science, Office of Nuclear Physics, under Award Number DE-AC05-00OR22725 and DOE DE-SC0014445

## References

- [1] N. Abgrall, et al., The Large Enriched Germanium Experiment for Neutrinoless  $\beta\beta$  Decay: LEGEND-1000 Preconceptual Design Report. [arXiv:2107.11462](#).
- [2] B. Abi, et al., The DUNE Far Detector Interim Design Report Volume 1: Physics, Technology and Strategies. [arXiv:1807.10334](#).
- [3] C. Cuesta, Status of ProtoDUNE Dual Phase, in: 2019 European Physical Society Conference on High Energy Physics, 2019. [arXiv:1910.10115](#).
- [4] Y. Efremenko, et al., Use of poly(ethylene naphthalate) as a self-vetoing structural material, JINST 14 (07) (2019) P07006. [arXiv:1901.03579](#), [doi:10.1088/1748-0221/14/07/P07006](#).
- [5] H. Nakamura, Y. Shirakawa, H. Kitamura, N. Sato, S. Takahashi, Detection of alpha particles with undoped poly (ethylene naphthalate), Nuclear Instruments and Methods in Physics Research Section A: Accelerators, Spectrometers, Detectors and Associated Equipment 739 (2014) 6–9.
- [6] L. Reichhart, D. Akimov, H. M. Araújo, E. J. Barnes, V. A. Belov, A. A. Burenkov, V. Chepel, A. Currie, L. DeViveiros, B. Edwards, V. Francis, C. Ghag, A. Hollingsworth, M. Horn, G. E. Kalmus, A. S. Kobayakin, A. G. Kovalenko, V. N. Lebedenko, A. Lindote, M. I. Lopes, R. Lüscher, P. Majewski, A. J. Murphy, F. Neves, S. M. Paling, J. Pinto da Cunha, R. Preece, J. J. Quenby, P. R. Scovell, C. Silva, V. N. Solovov, N. J. T. Smith, P. F. Smith, V. N. Stekhanov, T. J. Sumner, C. Thorne, R. J. Walker, Quenching factor for low-energy nuclear recoils in a plastic scintillator, Phys. Rev. C 85 (2012) 065801. [doi:10.1103/PhysRevC.85.065801](#).
- [7] Hamamatsu photomultiplier tubes and related products, [Online; accessed 27-March-2021].
- [8] L. G. Chiang, Nuclear materials identification system operational manual [doi:10.2172/814361](#).
- [9] Caen digitizer whitepaper - tools for discovery (Oct 2020).
- [10] D. L. Chichester, J. T. Johnson, E. H. Seabury, Measurement of the neutron spectrum of a DD electronic neutron generator [doi:10.1063/1.3586154](#).
- [11] V. Verbinski, W. Burrus, T. Love, W. Zobel, N. Hill, R. Textor, Calibration of an organic scintillator for neutron spectrometry, Nuclear Instruments and Methods 65 (1) (1968) 8–25. [doi:https://doi.org/10.1016/0029-554X\(68\)90003-7](#).